Development 139, 4374-4382 (2012) doi:10.1242/dev.084251

A conserved function for Strabismus in establishing planar cell polarity in the ciliated ectoderm during cnidarian larval development

Tsuyoshi Momose[1,2,*], Yulia Kraus[3] and Evelyn Houliston[1,2]

SUMMARY

Functional and morphological planar cell polarity (PCP) oriented along the oral-aboral body axis is clearly evident in the ectoderm of torpedo-shaped planula larvae of hydrozoan cnidarians such as *Clytia hemisphaerica*. Ectodermal epithelial cells bear a single motile cilium the beating of which is coordinated between cells, causing directional swimming towards the blunt, aboral pole. We have characterised PCP during *Clytia* larval development and addressed its molecular basis. PCP is first detectable in ectodermal cells during gastrulation as coordinated basal body positioning, the ciliary root becoming consistently positioned on the oral side of the apical surface of the cell. At later stages, more pronounced structural polarity develops around the base of each cilium in relation to the cilia beating direction, including a characteristic asymmetric cortical actin organisation. Morpholino antisense oligonucleotide and mRNA injection studies showed that PCP development requires the *Clytia* orthologues of the core Fz-PCP pathway components Strabismus (CheStbm), Frizzled (CheFz1) and Dishevelled (CheDsh). Morpholinos targeting any of these components prevented ectodermal PCP, disrupted ciliogenesis and inhibited embryo elongation during gastrulation, which involves cell intercalation. We show that YFP-tagged CheStbm adopts a polarised intracellular distribution, localising preferentially to the aboral boundary of each cell, as has been demonstrated in *Drosophila* and some vertebrate PCP studies. Our findings in a cnidarian strongly suggest that the Fz-PCP pathway is a highly conserved and evolutionary ancient metazoan feature that is probably widely responsible for oriented swimming and/or feeding in relation to body axis in the many ciliated larval types found throughout the animal kingdom.

KEY WORDS: Body axis, Cnidaria, Frizzled, Planar cell polarity, Strabismus/Van Gogh

INTRODUCTION

Planar cell polarity (PCP) is a key feature of many adult tissues. It accounts for the common orientation of epidermis-derived structures such as hairs, scales and feathers, and is also crucial for coordinating ciliary beating direction in many vertebrate epithelia, for example in airways and the kidney. The larval forms of most animal groups also bear ciliated ectodermal cells, the coordinated beating of which is responsible for directional swimming and/or feeding behaviour with respect to the main body axis (Jékely, 2011). For instance, cnidarian planula larvae are extensively covered by ciliated ectodermal cells aligned along the single oral-aboral axis (Fig. 1A), whereas lophotrochozoan (trochophore) and echinoderm (pluteus) larvae have ciliary bands positioned with respect to the mouth. Whether conserved PCP mechanisms acting in the ectoderm are responsible across the animal kingdom for allowing coordinated cilia beating in larvae is not known.

Our current understanding of the molecular basis of PCP establishment and orientation comes from extensive studies in *Drosophila* wing epithelia, abdomen and eye, and in a variety of vertebrate epithelial cells including the ciliated node cells that are active during mouse and zebrafish gastrulation (reviewed by Zallen, 2007; Seifert and Mlodzik, 2007; Wang and Nathans, 2007; Gray et al., 2011; Vladar et al., 2009). PCP development in these epithelia, i.e. the coordination of polarity between neighbouring cells, commonly requires a set of core PCP proteins: the transmembrane proteins Flamingo (Fmi), Frizzled (Fz) and Strabismus/Van Gogh (Stbm/Vang), and their cytoplasmic partners Dishevelled (Dsh), Prickle (Pk) and Diego (Dgo). These elements constitute the Fz-PCP pathway, which is often referred to as the Wnt-PCP pathway despite the non-obligatory participation of Wnt ligands. Most proposed mechanisms for core protein involvement in the Fz-PCP pathway place central importance on the differential localisation of Fz-Dsh-Dgo and Stbm-Pk protein complexes to opposing lateral boundaries of adjoining cells (reviewed by Zallen, 2007; Vladar et al., 2009; Gray et al., 2011). In *Drosophila* wing epithelial cells, the Fz-Dsh-Dgo complex becomes localised to the distal side of each cell and Stbm-Pk to the proximal side via interactions between adjacent cells mediated by the protocadherin Fmi (Starry night – FlyBase) (Chen et al., 2008). Similar asymmetric localisation of core PCP proteins has been observed in mouse inner ear hair cells (Montcouquiol et al., 2006; Wang et al., 2006; Deans et al., 2007). In vertebrates, core PCP proteins are also required for morphogenetic processes such as embryo elongation during gastrulation and neural tube closure, both involving convergent extension (CE) type cell movements (reviewed by Zallen, 2007; Simons and Mlodzik, 2008; Roszko et al., 2009). Asymmetric punctate protein localisation of Pk and Dsh has been observed during CE cell movements, albeit only in a faint and transient manner (Ciruna et al., 2006; Yin et al., 2008).

Despite the widespread occurrence of coordinated ciliary beating in larval ectoderm, the involvement of the Fz-PCP pathway has not been addressed. We thus aimed to describe in detail how PCP develops during gastrulation and larval development in the

[1]University of Pierre and Marie Curie, Developmental Biology Unit, Observatoire Océanologique, 06234 Villefranche-sur-mer, France. [2]CNRS, Developmental Biology Unit, 06234 Villefranche-sur-mer, France. [3]Department of Evolutionary Biology, Biological Faculty, Moscow State University, 119992, Moscow, Russia.

*Author for correspondence (tsuyoshi.momose@obs-vlfr.fr)

Accepted 30 August 2012

cnidarian experimental model *Clytia hemisphaerica*, a hydrozoan with a jellyfish form in its life cycle (Houliston et al., 2010), and to test the role of core PCP proteins. In cnidarians, as in many other metazoan groups, signalling through the canonical or Wnt/β-catenin pathway plays a decisive early role in embryonic axis establishment (Momose et al., 2008; Momose and Houliston, 2007; Wikramanayake et al., 2003). This leads to differential gene expression defining the identities of the future oral and aboral poles, including the activation of oral genes such as *Brachyury* (*CheBra*) required for cell ingression at gastrulation. In *Clytia*, the maternally expressed ligand CheWnt3 is required to activate Wnt/β-catenin signalling and thus oral gene expression, and is also required for embryo elongation (Momose et al., 2008), raising the possibility that Wnt3-directed activation of the Fz-PCP pathway might contribute to embryo elongation and ectodermal cell polarity. We now show that the *Clytia* orthologue of the core PCP protein Stbm (CheStbm) is essential to generate and coordinate PCP in the embryo and in planula larvae. CheStbm function promotes coordinated alignment of ciliated epidermal cells along the oral-aboral axis in gastrulating embryos and planula larvae, with CheStbm protein at the apical surface of each cell being localised preferentially to the aboral boundary. Two other PCP core components, CheDsh and CheFz1, are also required for this process. All three proteins also participate in embryo elongation, which, as in chordate embryonic axis elongation, involves cell intercalation orthogonal to the main body axis (Byrum, 2001). This study demonstrates strong functional conservation of the Fz-PCP pathway across the animal kingdom.

MATERIALS AND METHODS

Plasmid construction and mRNA synthesis

CheStbm mRNA was synthesised from a PCR product amplified from an EST clone (GenBank ID CU429033) with primers introducing the T3 promoter sequence and five point mutations in the morpholino antisense oligonucleotide (MO) target. mRNA for Stbm-YFP fusion protein was synthesised from our custom-made pCX3-Stbm-YFP vector, which includes short stretches of *CheStbm* 5′ and 3′ UTR sequences on either side of the cloning site. mRNA was synthesised in vitro using the mMessage mMachine T3 Kit (Ambion).

Microinjection

Clytia eggs and embryos were obtained from animals raised in the laboratory. Injection solutions were centrifuged briefly and injected into unfertilised eggs at ~1.5-3% egg volume prior to fertilisation within 1 hour of spawning, or injected into single blastomeres at the 2- to 8-cell stages. MO sequences (5′-3′) and injection concentrations were: Stbm-MO (CheStbm), TCACTCCATCATCAAAATCATCCAT, 0.32 mM; Control-MO (no target), CCTCTTACCTCAGTTACAATTTATA, 0.32 or 1 mM; Dsh-MO (CheDsh), TTAGTCTCTTTTTCAGCCATAACCC, 0.5 mM. Fz1-MO was described previously (Momose and Houliston, 2007). The concentrations of synthetic mRNAs were: *CheStbm*, 0.5 mg/ml; *Stbm-YFP*, 0.1 mg/ml. Alexa 647-labelled dextran (M_r ~7×10^4, Molecular Probes) was added to the injection solution for *CheStbm-YFP*.

Microinjections of mRNA for Stbm-YFP fusion protein at the dose used routinely (100 ng/μl) or even at higher dose (500 ng/μl, not shown) caused no visible perturbations of larval development or of PCP.

Fluorescent staining, microscopy and PCP quantification

Confocal imaging of morphology following phalloidin staining to detect polymerised actin structures including the cell cortex and following TO-PRO3 (Invitrogen) staining to label nuclei was as described previously (Momose and Houliston, 2007). Immunofluorescence (Amiel and Houliston, 2009) used anti-γ-tubulin antibody (GTU-88, Sigma-Aldrich) and Rhodamine-labelled anti-mouse secondary antibodies and post-staining with Alexa 488-labelled phalloidin (Invitrogen).

For PCP measurement, the top few micrometers from the apical surface of the ectodermal cells were imaged in a plane parallel to the apical surface using a Leica SP5 confocal microscope. The polarity of each cell was defined based on the position of the basal body (early gastrula stage) or the average direction of actin bundle distribution viewed from the basal body (later stages). For statistical analysis of the polarity distributions (see Fig. 3B,D,F), measurements were performed automatically using ImageJ software (NIH) and a plug-in script, applying the same criteria using ~300-500 cells observed in three to seven embryos. To score the degree of polarisation of each cell we calculated polarity indices. At the early gastrula stage the polarity index of each cell was defined as the distance between the centroid of its apical cell surface and the basal body, divided by its nominal radius (the radius of a circle with the same surface area). At planula stages a polarity index value was calculated to represent the angle covered by consecutive actin-positive areas around each basal body. At 180° the actin bundles form a semicircle and the index value is zero. The index value is 0.5 if actin bundles uniformly surround the basal body and –0.5 when there are no actin bundles.

In situ hybridisation and scanning electron microscopy (SEM)

In situ hybridisation procedures and the probes used were described previously (Momose and Houliston, 2007). CheStbm probe was transcribed from the EST clone SA0AAB22YG08 (GenBank ID CU429033) with T7 RNA polymerase. SEM was performed as described previously (Fritzenwanker et al., 2007).

RESULTS

PCP develops during primary embryonic axis establishment in *Clytia*

In the *Clytia* planula larva, the entire ectodermal epithelial layer exhibits clear oral-aboral tissue polarity in terms of cilia beating. The single cilium of each epithelial cell beats in a common direction along the oral-aboral axis, propelling the planula towards the blunt aboral pole (Fig. 1A). SEM confirmed the alignment of the cilia and revealed protruding microvilli, often asymmetrically arranged, at the base of each one (Fig. 1B), as described in other types of monociliated epithelial cells (Anstrom, 1992). To define reliable markers to monitor PCP development by confocal microscopy, we stained polymeric actin structures with fluorescent phalloidin in conjunction with anti-γ-tubulin immunofluorescence to visualise basal bodies (Fig. 1C).

Ciliogenesis in *Clytia* begins at the late blastula stage, when ectodermal cells have already developed a columnar shape and epithelial morphology. Basal bodies at this stage were found to be positioned close to the apical surface, but did not show regular positioning with respect to the oral-aboral axis or between the adjacent cells. At the early gastrula stage, when swimming starts and the oral-aboral axis was first discernible as a pointed oral gastrulation site where cell ingression starts, basal bodies were positioned towards the oral side of each ectodermal cell. The planar polarity of each cell at this stage could thus be defined by the position of its basal body. In 1- and 2-day planula larvae, basal body position was a less reliable polarity marker due to the reduced apical surface area of the epithelial cells; however, a pronounced asymmetry of the associated actin bundles on the aboral side of the basal bodies clearly indicated individual cell polarity. One or two tails of the γ-tubulin-positive ciliary rootlet (or basal foot) also projected from each basal body, pointing towards the aboral end below the actin bundles, as described previously in brain ependymal cells (Mirzadeh et al., 2010; Tsuji et al., 2010; Guirao et al., 2010).

Evaluation of PCP at successive embryonic stages revealed that the polarity of the ectodermal cells first became coordinated with that of neighbouring cells and aligned with the body axis at the early

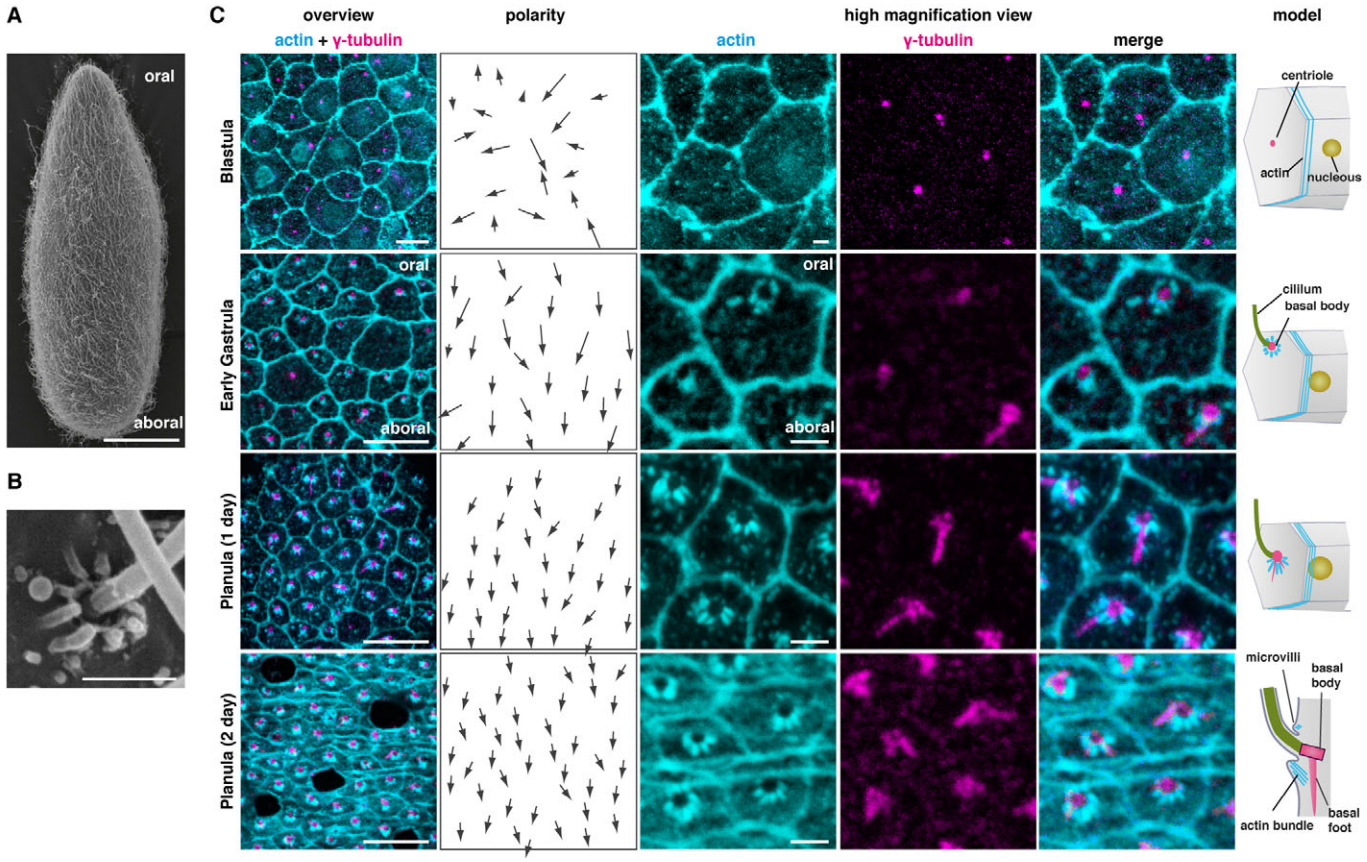

Fig. 1. PCP development in *Clytia* embryonic ectoderm. (**A**) Scanning electron micrograph of *Clytia* planula larva. Widespread ectodermal cilia beat directionally to promote aborally directed swimming. (**B**) High magnification of cilia and associated microvilli in a 2-day-old larva. (**C**) Ectodermal PCP in developing embryos and larvae. From left to right: confocal microscopy of F-actin and basal bodies stained with phalloidin and anti-γ-tubulin immunofluorescence near to the apical surface; vectorial representation of PCP determined from basal body position (blastula and early gastrula stages) or actin bundle distribution (planulae); high-magnification views of F-actin, γ-tubulin and merge; and drawings of PCP-related structures. Oral is at the top in all images, except for the blastula stages. Scale bars: 50 μm in A; 1 μm in B; 10 μm (overview) or 2 μm (high-magnification view) in C.

gastrula stage, concurrent with the first appearance of morphological oral-aboral polarity. PCP appeared globally across the embryo, with no obvious regional asynchrony in its development.

Clytia Stbm is expressed throughout embryogenesis and localises to aboral cell boundaries

We identified orthologues of all the core PCP proteins in our *Clytia* transcriptomic sequence collection (Forêt et al., 2010), with the exception of Four-jointed (Table 1); nor was a Four-jointed orthologue identifiable in the fully sequenced genomes of *Hydra* and *Nematostella*, suggesting that this gene might be absent from all Cnidaria. To attempt to intervene in PCP development in *Clytia* we focused on the Stbm orthologue CheStbm. Studies in vertebrates and *Drosophila* indicate that Stbm specifically regulates PCP and, unlike Fz and Dsh, plays no direct role in Wnt/β-catenin signalling. *CheStbm* mRNA was detected uniformly in the embryo from the egg to planula stages, i.e. before and during PCP establishment (Fig. 2A). In 1-day planulae, a slight aboral-oral gradient of *CheStbm* mRNA was apparent, opposite to the *CheFz1* mRNA gradient (Momose and Houliston, 2007).

To assess the localisation of CheStbm protein by confocal microscopy, we injected mRNA encoding a CheStbm-YFP fusion protein prior to fertilisation. At the early gastrula stage, the YFP signal in ectodermal cells was concentrated around the cell boundaries near the apical cell surface (Fig. 2B). Polarity in its intracellular distribution was difficult to assess in these embryos because of the close apposition of the signals from adjoining cells. We thus introduced the mRNA together with a fluorescent dextran linage tracer into single blastomeres of 4- or 8-cell stage embryos and focussed on the boundaries between the descendants of injected and non-injected blastomeres. First, we examined cells at the oral edge of Stbm-YFP-expressing patches (Fig. 2C, left panels). In this situation, 19 out of 20 cells examined showed YFP signal at the aboral boundary (i.e. the boundary neighbouring other Stbm-YFP-expressing cells) but not at the oral boundary. The one exception showed YFP signal all around the cell periphery. Second, we examined cells on the aboral edge of Stbm-YFP-expressing patches (Fig. 2C, right panels). All nine cells showed YFP fluorescence on the aboral side, despite the absence of YFP in the adjoining cell. Signal intensity at the oral side was harder to assess due to close proximity of Stbm-YFP in the adjoining cells, but in four cases the YFP signal appeared absent or reduced. Finally, four Stbm-YFP-expressing cells were identified that lacked fluorescent neighbours on both oral and aboral sides. In all four cases, YFP

Table 1. *Clytia* orthologues of core PCP proteins

Orthologue	*Drosophila*	Vertebrate	*Clytia*	GenBank ID	Domain structures (N- to C-terminus) or sequence similarity to *Drosophila* protein
Stbm	Van Gogh [Vang; Strabismus (Stbm)]	Vang-like 1, 2 (Vangl1, 2)	CheStbm	JQ439008	Almost entire region is conserved with Van Gogh; five-pass transmembrane domain near N-terminus
Pk	Prickle (Pk)	Prickle-like 1, 2 (Prickle1, 2)	ChePk	JQ439007	Prickle PET domain followed by three LIM domains
Fz	Frizzled (Fz)	Frizzled 3, 6, 7 (Fzd3, 6, 7)	CheFz1	DQ869571	Orthologue of Fz in Drosophila and Fzd127/36 group in vertebrates
Dsh	Dishevelled (Dsh)	Dishevelled 1-3 (Dvl1-3)	CheDsh	JQ439000	DAX, PDZ and DEP domains
Fmi	Flamingo [Fmi; Starry night (Stan)]	Celsr1-3	CheFmi	JQ439002	Eight cadherin repeats followed by Fmi box, five EGF domains and two laminin G motifs, seven-pass transmembrane domain
Dgo	Diego (Dgo)	Inversin (Invs)	CheDgo	JQ438998	PET domain followed by 16 Ankyrin repeats then three LIM domains
Fy	Fuzzy (Fy)	Fuzzy (Fuz)	CheFy	JQ439003	Almost entire region is conserved with Fy (query coverage 90%, maximum identity 30%)
In	Inturned (In)	Inturned (Intu)	CheIn	JQ439006	PDZ domain near the N-terminus; large part of the sequence is conserved with In (query coverage 70%, maximum identity 21%)
Fat	Fat (Ft)	Fat1-4	CheFat	JQ439001	Partial cDNA with missing 5′ sequence; at least 18 cadherin repeats followed by weak similarity to Fmi box; seven EGF and one laminin G motif; single transmembrane domain
Dachsous	Dachsous (Ds)	Dachsous 1, 2 (Dchs1, 2)	CheDach	JQ438998	Twenty-seven cadherin repeats followed by transmembrane domain
Four-jointed	Four-jointed (Fj)	Four jointed box 1 (Fjx1)	None	–	Not found in Hydra or Nematostella whole-genome sequences

could be detected only at the aboral boundary. Together, these observations demonstrate that CheStbm protein preferentially localises at the aboral boundary of each ectodermal cell.

Roles for CheStbm in PCP and ciliogenesis

To test the function of CheStbm, we introduced by microinjection a morpholino antisense oligonucleotide (Stbm-MO) designed to block translation from *CheStbm* mRNA. No effect on cell division, cellular organisation or overall development was observed in Stbm-MO embryos before the gastrula stage, and the development of epithelial organisation (apical-basal polarity) of the ectodermal layer occurred normally. PCP, as assessed by determining basal body position (early gastrula) or orientation of actin bundle distribution (1-day larva), was severely disturbed at both stages in embryos derived from Stbm-MO-injected eggs (Fig. 3A). The specificity of the Stbm-MO was confirmed by reversing the phenotype by subsequent injection of synthetic *Stbm* mRNA bearing five neutral point mutations in the MO target; coordinated PCP in the resulting rescued embryos was virtually indistinguishable from that of non-injected embryos (Fig. 3A).

Quantification of PCP in either early gastrulae (basal body position) or 1-day planulae (actin bundle distribution) revealed that, whereas the orientation of individual cells in non-injected embryos almost always fell within 45° of the average PCP axis (Fig. 3B), cells in Stbm-MO embryos were oriented in all directions, with only a residual trace of common alignment (Fig. 3B). Not only was PCP coordination between cells severely compromised, but also some individual cells completely failed to develop PCP, their basal bodies being positioned at the centre of the apical cell surface (Fig. 3C). The average distance between a basal body and the centroid of the apical surface area of each cell (excluding mitotic cells) was thus significantly reduced in Stbm-MO-injected embryos and restored in rescued embryos (Fig. 4D). Similarly, in 1-day larvae, the actin structures became uniformly distributed around basal bodies in some cells (Fig. 3E), increasing the angle of actin bundles around the basal body (Fig. 3F). Injection of *Stbm* mRNA into Stbm-MO embryos effectively restored PCP, the distribution of actin structures around each basal body becoming even narrower than in non-injected planula.

Stbm-MO embryos showed defects not only in PCP, but also in ciliogenesis itself (Fig. 3G). SEM revealed regions in the ectoderm where cells lacked cilia. A residual hole surrounded by the microvilli could sometimes be detected. Other regions showed shorter and/or curled cilia, highly reminiscent of the defects observed following perturbation of core PCP proteins in vertebrate studies (Park et al., 2006).

From these observations we conclude that CheStbm is required for PCP coordination along the primary body axis during *Clytia* embryogenesis, that it favours the development of individual cell polarity in terms of basal body position and of structural asymmetry around the ciliary base, and promotes ciliogenesis itself.

CheStbm contributes to embryo elongation and axial gene expression

During normal *Clytia* embryogenesis, the elongated shape of the planula larva develops during gastrulation in parallel with the ingression of presumptive endodermal cells from the oral pole (Fig. 4A). In addition to disruption of PCP and ciliogenesis, Stbm-MO embryos showed two morphogenesis defects relating to these processes: severely reduced elongation along the oral-aboral axis and an expanded gastrulation initiation site. Virtually no elongation occurred during gastrulation, while cell ingression proceeded from a wider than usual site to produce nearly, but not entirely, spherical embryos (Fig. 4A,B). Following gastrulation, Stbm-MO embryos elongated slightly but never attained the length of uninjected controls.

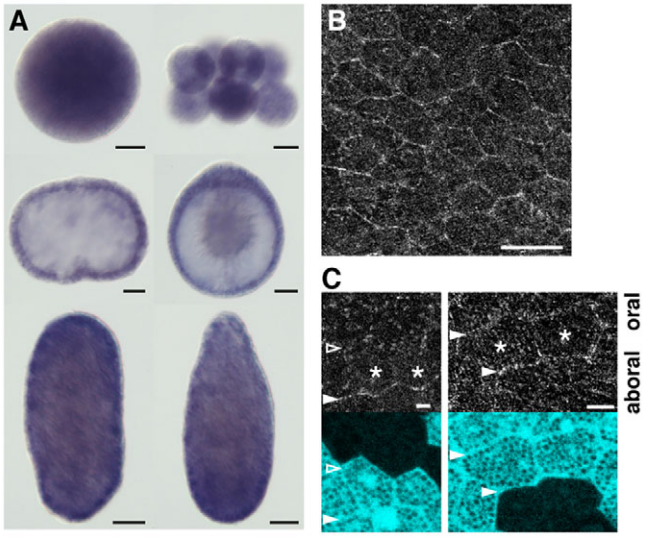

Fig. 2. CheStbm protein localises aborally. (**A**) In situ hybridisation of *CheStbm* mRNA during embryonic development. From top left to bottom right: egg, 8-cell stage, blastula, early gastrula, late gastrula and 1-day-old planula. (**B**) Distribution of CheStbm-YFP fusion protein at the apical surface of ectoderm at the early gastrula stage following mRNA injection into the egg. (**C**) CheStbm-YFP distribution (top panels) following co-injection of mRNA with dextran-Alexa 647 (bottom panels) into one or two blastomeres at the 4-cell stage. Asterisks indicate CheStbm-YFP-positive cells adjoining negative cells on the oral (left) and aboral (right) sides, with filled and open arrowheads respectively marking the boundary between these cells and those expressing CheStbm-YFP or not. Oral pole of embryo is to the top. The weakness of the YFP signal is partly due to imaging difficulties caused by endogenous GFP proteins naturally expressed in *Clytia* eggs and embryos; to discriminate YFP from endogenous GFP requires narrowing the detection bandwidth, eliminating a large part of the signal. Scale bars: 50 μm in A; 10 μm in B; 2 μm in C.

We hypothesised that the embryo elongation defect in Stbm-MO embryos could be a direct consequence of PCP disruption. Consistent with this hypothesis, equivalent phenotypes of both PCP and embryo elongation were observed following injection of MOs targeting the translation of two other core PCP molecules: CheFz1 (Momose and Houliston, 2007) and the Dsh orthologue CheDsh (Fig. 5). In the North American *Clytia* (*Phialidium*) species *C. gregarium* (Byrum, 2001), analysis of the shape of clones of ectodermal cells indicated that lateral intercalation occurs orthogonal to the oral-aboral axis during gastrulation. Lateral cell intercalation has also been shown to occur during epithelial evagination and elongation during *Hydra* budding (Philipp et al., 2009). These cell reorganisations during morphogenesis in cnidarians are reminiscent of the CE movements of involuting mesoderm cells perpendicular to the anterior-posterior axis during vertebrate gastrulation, a process that is dependent on the Fz-PCP pathway and inhibited by Stbm knockdown in *Xenopus* and zebrafish (Park and Moon, 2002; Darken et al., 2002; Goto and Keller, 2002). The pattern of contacts between ectodermal cells in *Clytia* embryos fixed at the early gastrula stage is consistent with lateral displacement of ectodermal cells (Fig. 4C): the oral/aboral interfaces between ectodermal cells are aligned, whereas their lateral boundaries are not, most notably in regions close to the pointed oral end of the embryo. Further studies are clearly required to confirm and fully characterise cell movement during *Clytia* embryo elongation.

To explain the observed expansion of the gastrulation initiation site in Stbm-MO embryos (Fig. 4A,B) we hypothesised that the domains of expression of oral-specific genes, such as the *Brachyury* orthologue *CheBra*, might be less restricted than in unmanipulated embryos. CheBra expression is dependent on activation of the Wnt/β-catenin pathway for transcriptional regulation through the ligand CheWnt3 and the receptor CheFz1 (Momose et al., 2008; Momose and Houliston, 2007). We monitored by in situ hybridisation the expression of *CheBra* and of the aborally expressed transcription factor gene *CheFoxQ2a* (Fig. 4D) in Stbm-MO embryos. Consistent with the expanded gastrulation site, the *CheBra* expression domain was expanded in Stbm-MO embryos from the early gastrula stage through to planula formation. Conversely, aboral *FoxQ2a* expression was significantly delayed in Stbm-MO embryos, being completely undetectable at the early gastrula stage but then becoming re-established by the end of gastrulation. These observations suggest that CheStbm, possibly via the Fz-PCP pathway, exerts an inhibitory effect on Wnt/β-catenin signalling, at least during the early stages of gastrula patterning.

DISCUSSION

We have described in detail the development of PCP during embryonic axis formation in the cnidarian *Clytia hemisphaerica*, and performed functional studies demonstrating highly conserved involvement of the Fz-PCP pathway. Ectodermal PCP in *Clytia* was first detectable at the early gastrula stage, concurrent with ciliogenesis. It was first manifest as asymmetric positioning of the basal body towards the oral side in the cell, and later as a characteristic polarised actin organisation surrounding the ciliary rootlet. We showed that establishment of ectodermal PCP in *Clytia* larvae requires highly conserved Fz-PCP pathway components (core PCP proteins). Thus, experimental downregulation of *Clytia* orthologues of Stbm/Vang, Fz and Dsh resulted in strikingly similar phenotypes to those described in *Drosophila* and vertebrate studies: disrupted PCP coordination, loss of cell polarisation, and ciliogenesis defects. Furthermore, we found that, as in *Drosophila*, *Clytia* Stbm protein is apically concentrated in ectodermal cells and preferentially localised at the aboral boundary. Finally, we demonstrated that Stbm, Fz and Dsh functions contribute to embryo elongation in *Clytia*, suggesting that the Fz-PCP pathway might participate in morphogenesis during gastrulation as it does in vertebrates. These findings in a cnidarian imply a very ancient evolutionary origin for the Fz-PCP pathway in metazoans and show that the Fz-Stbm-Dsh core mechanism has been highly conserved during the evolution of phylogenetically distant animal lineages.

Stbm as an ancient and conserved PCP regulator

The Fz-PCP system for tissue polarity appears to be a metazoan innovation (Lapébie et al., 2011). Genes for Fz, Fmi and Dsh are present across metazoan genomes, including sponges, but are not detectable in the genomes of unicellular relatives or in other multicellular organisms. Pk and Dgo, however, are identifiable in choanoflagellates, suggesting roles predating multicellularity. These roles could have been related to ciliogenesis, asymmetric basal body positioning or basal body anchoring, which are emerging as being strongly linked to Fz-mediated PCP mechanisms across diverse vertebrate models, including ciliated node cells in mouse, *Xenopus* and zebrafish gastrulae, *Xenopus* multiciliated epidermis and mouse brain ventricular ependymal cells (reviewed by Hashimoto and Hamada, 2010; Wallingford, 2010; Bayly and Axelrod, 2011; Wallingford and Mitchell, 2011). Cell polarity in

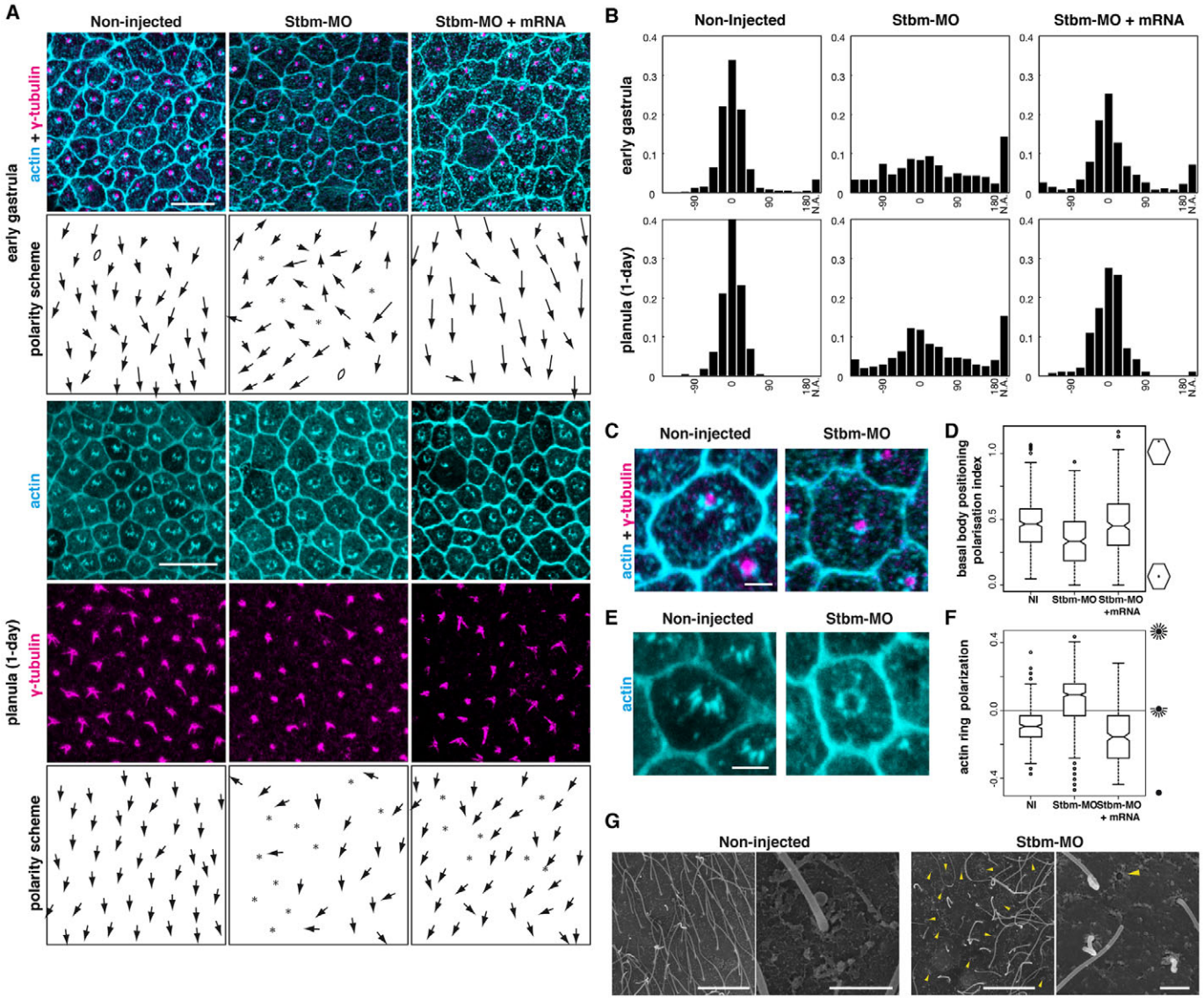

Fig. 3. CheStbm-MO abolishes PCP. (**A**) PCP in *Clytia* early gastrula embryos (top two rows) and 1-day-old planula larvae (bottom three rows) monitored by basal body position and distribution of actin bundle in non-injected controls, Stbm-MO-injected embryos, and with Stbm-MO injection followed by *CheStbm* mRNA injection. Asterisks in the polarity scheme indicate cells with no clear polarity. (**B**) Polarity distribution in A. Angles of cell polarity with respect to oral-pointing in non-injected embryos (0 degrees) are grouped in 22.5° intervals. N.A., cells without measurable polarity. (**C**) Early gastrula cells lacking asymmetric basal body positioning. (**D**) Notched box-plot showing the polarity index distribution in early gastrula cells. (**E**) One-day-old planula cells with uniform distribution of actin bundles. (**F**) Notched box-plot of the cell polarity index distribution in 1-day-old planulae. (**G**) SEM of cilia formation. Arrowheads indicate traces of cilia surrounded by microvilli. (D,F) Whiskers represent 1.5 interquartile range and the notches indicate 95% confidence interval of the median. NI, non-injected. Oral is to the top in non-injected and rescued embryos. Scale bars: 10 µm in A,G (low magnification); 2 µm in C,E,G (high magnification).

the *Clytia* larva ectodermal plane is manifest in two main ways relating to the coordination of ciliary beating between cells. As described in mouse brain ventricle cells and precursor glial cells (Mirzadeh et al., 2010), positioning of the basal body in each *Clytia* gastrula ectodermal cell (translational polarity) precedes the development of asymmetry in the actin and ciliary rootlet structures around the basal body (rotational polarity), suggesting that similar mechanisms are employed for constructing polarity in ciliated epithelium in mice and *Clytia*. It seems reasonable to propose that the earliest multicellular animals used the core PCP proteins inherited from flagellated unicellular ancestors to structure the basal body environment asymmetrically in relation to ciliary beating direction, acquiring novel extracellular interactions, for instance between Stbm and Fz, to coordinate this process between cells. Our observations in *Clytia* imply that Fz-PCP signalling was already employed by the eumetazoan (cnidarian plus bilaterian) common ancestor, and perhaps by a common ancestor of all metazoa.

Stbm and the other core PCP proteins are clearly essential mediators of PCP in *Drosophila* and in vertebrates, with strong evidence from *Drosophila* and weaker evidence from vertebrate epithelial PCP systems that reciprocal localisation of the two key protein complexes to opposite cell boundaries is a key feature of PCP. Our study of CheStbm is the first demonstration that a core

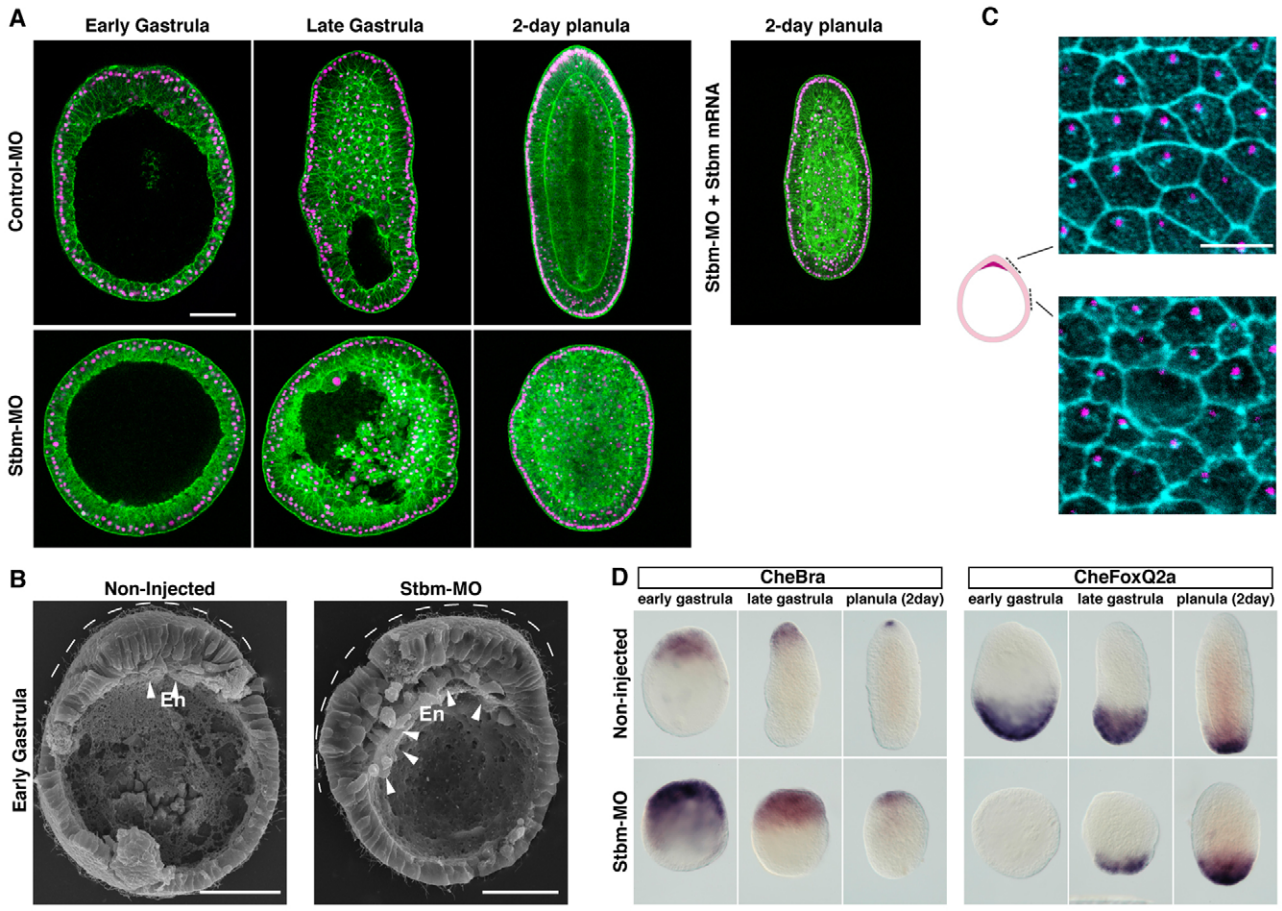

Fig. 4. CheStbm participates in embryo elongation. (**A**) Confocal microscopy of *Clytia* embryo morphology visualised with actin (green) and nuclei (magenta) staining. (**B**) Endoderm formation in early gastrulae observed by SEM in non-injected and Stbm-MO-injected embryos. Arrowheads indicate presumptive endodermal cells migrating into the blastocoel. En, endoderm. Dashed line indicates the region in which the endoderm ingression was observed. (**C**) Apical cell contours in oral and medial regions of an early gastrula embryo visualised by confocal imaging of actin (cyan) and basal bodies (magenta). (**D**) Expression of *CheBra* (oral) and *FoxQ2a* (aboral) detected by in situ hybridisation. Oral is to the top. Scale bars: 50 μm in A,B; 10 μm in C.

PCP protein localises asymmetrically and is essential for epithelial tissue polarity in a non-bilaterian animal, indeed in any experimental system outside *Drosophila* and vertebrates. Surprisingly little is known about the function of core PCP proteins in other animal groups. In planarians, the orthologue (Smed-dvl-2) of Dsh, a component that participates in both Fz-PCP and Wnt/β-catenin signalling, is required for apical basal body anchoring and cilia formation (Almuedo-Castillo et al., 2011), consistent with the hypothesis of a conserved role for core PCP proteins in structuring polarised epithelia. In *Hydra* polyps, a possible involvement of non-canonical (i.e. β-catenin-independent) Wnt signalling in bud and tentacle morphogenesis was suggested by studies using a pharmacological inhibitor of Jun N-terminal kinase (JNK) (Philipp et al., 2009), which mediates morphogenetic processes. Some of these morphogenetic processes are regulated by the Fz-PCP pathway (Lapébie et al., 2011). Potential functions in PCP regulation of the candidate Wnt signalling regulators identified in the *Hydra* study remain to be tested. A study of the Stbm orthologue (NvStbm) in the anthozoan cnidarian *Nematostella vectensis* showed marked localisation of its mRNA and protein in the fertilised egg and early embryo, something we did not see in *Clytia*, and uncovered a β-catenin-independent role in epithelial invagination at the onset of archenteron formation (Kumburegama et al., 2011), which may be related to PCP (see below). No defects in PCP in ciliated ectoderm or elongation were noted following NvStbm MO injection (Kumburegama et al., 2011). This might be due to heterochrony between tissue polarity development and other processes including gastrulation in *Nematostella vectensis*, or simply because ectodermal PCP was not specifically assayed.

PCP and embryo morphogenesis

We have argued above that the Fz-PCP pathway probably arose in ancestral metazoans to generate planar tissue polarity in ciliated epithelia to favour directed swimming. PCP development along the principal body axis in the early embryo might have had important consequences for body plan evolution by allowing coordination of cell behaviours during morphogenetic processes, such as gastrulation and elongation, along the body axis. In chordates, including vertebrates and ascidians, PCP core proteins participate in morphogenetic processes, notably the polarised convergence of involuting mesoderm cells during gastrulation that is responsible for embryo elongation (Jiang et al., 2005; Zallen, 2007; Simons and Mlodzik, 2008; Roszko et al., 2009). In *Clytia*, CheStbm and CheFz1 participate in elongation along the oral-aboral axis, a

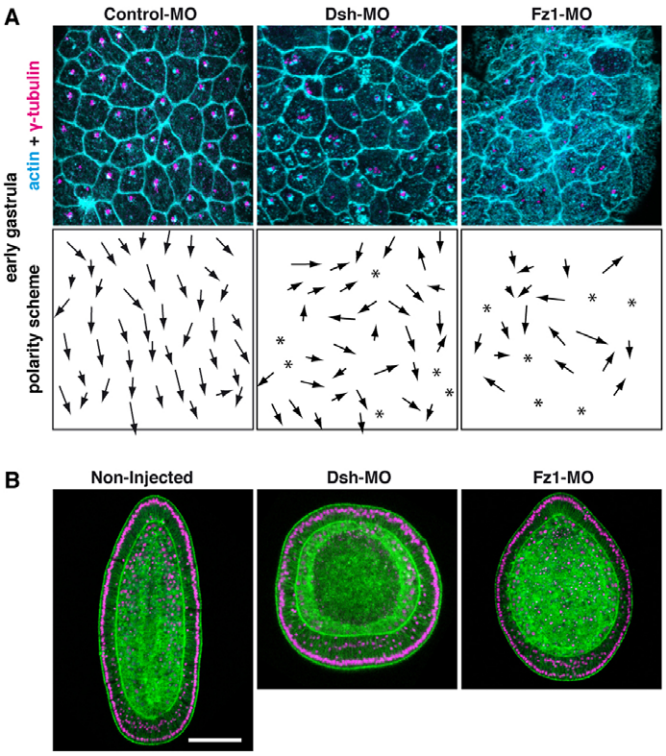

Fig. 5. CheDsh and CheFz1 are required for PCP coordination. (**A**) PCP in Dsh-MO-injected or Fz1-MO-injected early gastrula *Clytia* embryos, monitored by basal body position. In both cases, more than two basal bodies were seen in a single cell. PCP was partially restored in 1-day-old planula larvae (data not shown). (**B**) Morphology of Dsh-MO-injected or Fz1-MO-injected 2-day-old planula larvae monitored by confocal microscopy as described in Fig. 4A. Scale bar: 50 μm.

process that appears to resemble CE in that it involves cell intercalation, as revealed by cell lineage-tracing studies (Byrum, 2001). The cellular mechanisms underlying elongation remain largely unclear however, and may also involve directional cell division (Gong et al., 2004) or the elongation of individual cells. The migration of endoderm cells during gastrulation and possibly their subsequent reorganisation into an epithelial layer might also contribute to embryo elongation in *Clytia*. Endoderm-driven elongation is, however, unlikely to be a common mechanism in cnidarians because other hydrozoans such as *Podocoryne carnea* undergo embryo elongation before any cell ingression occurs (Momose and Schmid, 2006).

In the study of *Nematostella* NvStbm (Kumburegama et al., 2011), no defects in body elongation or coordinated cell polarity were reported following MO knockdown. Archenteron formation through tissue invagination was, however, inhibited. This defect might reflect a requirement for PCP in coordinating the morphogenetic cell behaviour of epithelial folding, as has been proposed to explain neural tube closure defects in mouse *Loop-tail* (*Vangl2*, an *Stbm* orthologue) mutants (Kibar et al., 2001; Murdoch et al., 2001). *Clytia* gastrulation differs from that of *Nematostella*, with endoderm forming not by tissue sheet invagination but by ingression of individual cells, followed by their epithelialisation at a later stage. The difference in the Stbm-MO phenotypes in the two cnidarians might therefore simply reflect the different modes of gastrulation. Supporting this view, invagination of the epithelial archenteron in sea urchin is blocked by experimental interference with PCP components using specific dominant-negative forms of Fz5/8 (extracellular domain) or of Dsh (DEP domain) (Croce et al., 2006; Byrum et al., 2009). Morphogenesis controlled by conserved core PCP proteins therefore appears to be a common feature of metazoan development, but its precise involvement might have changed during animal evolution depending on the varying contribution of different cellular processes to the morphogenetic events of embryogenesis.

Coupling of Wnt and Fz-PCP signalling during axis specification

Wnt/β-catenin signalling is employed in species right across the metazoan tree for germ layer and/or axis specification during early embryonic development, consistently prefiguring the site of gastrulation and of endomesoderm formation (Logan et al., 1999; Wikramanayake et al., 2003; Momose and Houliston, 2007; Momose et al., 2008; Petersen and Reddien, 2009; Darras et al., 2011) (reviewed by Henry et al., 2008). It is thus likely to have been ancestrally involved in generating the earliest asymmetries in gene expression in developing embryos. Our study establishes that the Fz-PCP pathway is probably also an ancestral metazoan feature. This raises the interesting possibility that the Fz-PCP pathway and Wnt/β-catenin-dependent axis specification could have been coordinated in early metazoans by the participation of a common Wnt ligand. In this scenario, the ancestral situation would have been retained in *Clytia*, where a single Wnt ligand, CheWnt3, is expressed prior to gastrulation and then remains expressed at the oral pole of the embryo (Momose et al., 2008). CheWnt3 is essential for Wnt/β-catenin pathway activation and is positioned appropriately to provide a directional cue to orient PCP during gastrulation. Consistent with this hypothesis, CheWnt3-MO-injected embryos fail to attain the elongated torpedo shape (Momose et al., 2008). It remains to be established whether the implied disorganisation of PCP in these embryos is a direct consequence of the absence of the Wnt3 ligand or of downstream Wnt/β-catenin signalling target genes.

How Wnt ligands act to orient PCP globally remains much debated and appears to vary between species. In *Drosophila*, global PCP orientation is directed by gradients of Dachsous/Four-jointed in wing and eye, and additionally by Fz in the abdomen (reviewed by Lawrence et al., 2007), with the Wnt ligand not being required in wing and abdomen PCP (Lawrence et al., 2002; Chen et al., 2008). In the mouse inner ear, Wnt sources can orient PCP but the mechanism is unclear (Qian et al., 2007; Dabdoub et al., 2003). In mouse limb cartilage, a Wnt gradient acts via the unconventional receptor Ror2 to generate a gradient of phosphorylated Vangl2 (Stbm) protein (Bingham et al., 2010), but it is not clear whether its role is to orient or to coordinate PCP. *Clytia* embryos could provide a simple new model with which to study the role of Wnt ligands in orienting PCP.

Acknowledgements
We thank our research colleagues for stimulating discussions and EM laboratory of Moscow State University for technical support.

Funding
This work was supported by the Agence Nationale de la Recherche (ANR) Programme Blanc ['DiploDevo' to T.M. and E.H.] and by a Subvention Fixé from the Foundation ARC pour la Recherche sur le Cancer [ARC1098 to T.M.].

Competing interests statement
The authors declare no competing financial interests.

Author contributions
Y.K. performed SEM imaging and T.M. performed all other experiments. T.M. and E.H. wrote the manuscript.

References

Almuedo-Castillo, M., Saló, E. and Adell, T. (2011). Dishevelled is essential for neural connectivity and planar cell polarity in planarians. *Proc. Natl. Acad. Sci. USA* **108**, 2813-2818.

Amiel, A. and Houliston, E. (2009). Three distinct RNA localization mechanisms contribute to oocyte polarity establishment in the cnidarian Clytia hemisphaerica. *Dev. Biol.* **327**, 191-203.

Anstrom, J. A. (1992). Organization of the ciliary basal apparatus in embryonic cells of the sea urchin, Lytechinus pictus. *Cell Tissue Res.* **269**, 305-313.

Bayly, R. and Axelrod, J. D. (2011). Pointing in the right direction: new developments in the field of planar cell polarity. *Nat. Rev. Genet.* **12**, 385-391.

Bingham, S. M., Sittaramane, V., Mapp, O., Patil, S., Prince, V. E. and Chandrasekhar, A. (2010). Multiple mechanisms mediate motor neuron migration in the zebrafish hindbrain. *Dev. Neurobiol.* **70**, 87-99.

Byrum, C. A. (2001). An analysis of hydrozoan gastrulation by unipolar ingression. *Dev. Biol.* **240**, 627-640.

Byrum, C. A., Xu, R., Bince, J. M., McClay, D. R. and Wikramanayake, A. H. (2009). Blocking Dishevelled signaling in the noncanonical Wnt pathway in sea urchins disrupts endoderm formation and spiculogenesis, but not secondary mesoderm formation. *Dev. Dyn.* **238**, 1649-1665.

Chen, W.-S., Antic, D., Matis, M., Logan, C. Y., Povelones, M., Anderson, G. A., Nusse, R. and Axelrod, J. D. (2008). Asymmetric homotypic interactions of the atypical cadherin flamingo mediate intercellular polarity signaling. *Cell* **133**, 1093-1105.

Ciruna, B., Jenny, A., Lee, D., Mlodzik, M. and Schier, A. F. (2006). Planar cell polarity signalling couples cell division and morphogenesis during neurulation. *Nature* **439**, 220-224.

Croce, J., Duloquin, L., Lhomond, G., McClay, D. R. and Gache, C. (2006). Frizzled5/8 is required in secondary mesenchyme cells to initiate archenteron invagination during sea urchin development. *Development* **133**, 547-557.

Dabdoub, A., Donohue, M. J., Brennan, A., Wolf, V., Montcouquiol, M., Sassoon, D. A., Hseih, J.-C., Rubin, J. S., Salinas, P. C. and Kelley, M. W. (2003). Wnt signaling mediates reorientation of outer hair cell stereociliary bundles in the mammalian cochlea. *Development* **130**, 2375-2384.

Darken, R. S., Scola, A. M., Rakeman, A. S., Das, G., Mlodzik, M. and Wilson, P. A. (2002). The planar polarity gene strabismus regulates convergent extension movements in Xenopus. *EMBO J.* **21**, 976-985.

Darras, S., Gerhart, J., Terasaki, M., Kirschner, M. and Lowe, C. J. (2011). β-catenin specifies the endomesoderm and defines the posterior organizer of the hemichordate Saccoglossus kowalevskii. *Development* **138**, 959-970.

Deans, M. R., Antic, D., Suyama, K., Scott, M. P., Axelrod, J. D. and Goodrich, L. V. (2007). Asymmetric distribution of prickle-like 2 reveals an early underlying polarization of vestibular sensory epithelia in the inner ear. *J. Neurosci.* **27**, 3139-3147.

Forêt, S., Knack, B., Houliston, E., Momose, T., Manuel, M., Quéinnec, E., Hayward, D. C., Ball, E. E. and Miller, D. J. (2010). New tricks with old genes: the genetic bases of novel cnidarian traits. *Trends Genet.* **26**, 154-158.

Fritzenwanker, J. H., Genikhovich, G., Kraus, Y. and Technau, U. (2007). Early development and axis specification in the sea anemone Nematostella vectensis. *Dev. Biol.* **310**, 264-279.

Gong, Y., Mo, C. and Fraser, S. E. (2004). Planar cell polarity signalling controls cell division orientation during zebrafish gastrulation. *Nature* **430**, 689-693.

Goto, T. and Keller, R. (2002). The planar cell polarity gene strabismus regulates convergence and extension and neural fold closure in Xenopus. *Dev. Biol.* **247**, 165-181.

Gray, R. S., Roszko, I. and Solnica-Krezel, L. (2011). Planar cell polarity: coordinating morphogenetic cell behaviors with embryonic polarity. *Dev. Cell* **21**, 120-133.

Guirao, B., Meunier, A., Mortaud, S., Aguilar, A., Corsi, J.-M., Strehl, L., Hirota, Y., Desoeuvre, A., Boutin, C., Han, Y.-G. et al. (2010). Coupling between hydrodynamic forces and planar cell polarity orients mammalian motile cilia. *Nat. Cell Biol.* **12**, 341-350.

Hashimoto, M. and Hamada, H. (2010). Translation of anterior-posterior polarity into left-right polarity in the mouse embryo. *Curr. Opin. Genet. Dev.* **20**, 433-437.

Henry, J. Q., Perry, K. J., Wever, J., Seaver, E. and Martindale, M. Q. (2008). Beta-catenin is required for the establishment of vegetal embryonic fates in the nemertean, Cerebratulus lacteus. *Dev. Biol.* **317**, 368-379.

Houliston, E., Momose, T. and Manuel, M. (2010). Clytia hemisphaerica: a jellyfish cousin joins the laboratory. *Trends Genet.* **26**, 159-167.

Jékely, G. (2011). Origin and early evolution of neural circuits for the control of ciliary locomotion. *Proc. Biol. Sci.* **278**, 914-922.

Jiang, D., Munro, E. M. and Smith, W. C. (2005). Ascidian prickle regulates both mediolateral and anterior-posterior cell polarity of notochord cells. *Curr. Biol.* **15**, 79-85.

Kibar, Z., Vogan, K. J., Groulx, N., Justice, M. J., Underhill, D. A. and Gros, P. (2001). Ltap, a mammalian homolog of Drosophila Strabismus/Van Gogh, is altered in the mouse neural tube mutant Loop-tail. *Nat. Genet.* **28**, 251-255.

Kumburegama, S., Wijesena, N., Xu, R. and Wikramanayake, A. H. (2011). Strabismus-mediated primary archenteron invagination is uncoupled from Wnt/β-catenin-dependent endoderm cell fate specification in Nematostella vectensis (Anthozoa, Cnidaria): Implications for the evolution of gastrulation. *Evodevo* **2**, 2.

Lapébie, P., Borchiellini, C. and Houliston, E. (2011). Dissecting the PCP pathway: one or more pathways?: Does a separate Wnt-Fz-Rho pathway drive morphogenesis? *BioEssays* **33**, 759-768.

Lawrence, P. A., Casal, J. and Struhl, G. (2002). Towards a model of the organisation of planar polarity and pattern in the Drosophila abdomen. *Development* **129**, 2749-2760.

Lawrence, P. A., Struhl, G. and Casal, J. (2007). Planar cell polarity: one or two pathways? *Nat. Rev. Genet.* **8**, 555-563.

Logan, C. Y., Miller, J. R., Ferkowicz, M. J. and McClay, D. R. (1999). Nuclear beta-catenin is required to specify vegetal cell fates in the sea urchin embryo. *Development* **126**, 345-357.

Mirzadeh, Z., Han, Y.-G., Soriano-Navarro, M., García-Verdugo, J. M. and Alvarez-Buylla, A. (2010). Cilia organize ependymal planar polarity. *J. Neurosci.* **30**, 2600-2610.

Momose, T. and Houliston, E. (2007). Two oppositely localised frizzled RNAs as axis determinants in a cnidarian embryo. *PLoS Biol.* **5**, e70.

Momose, T. and Schmid, V. (2006). Animal pole determinants define oral-aboral axis polarity and endodermal cell-fate in hydrozoan jellyfish Podocoryne carnea. *Dev. Biol.* **292**, 371-380.

Momose, T., Derelle, R. and Houliston, E. (2008). A maternally localised Wnt ligand required for axial patterning in the cnidarian Clytia hemisphaerica. *Development* **135**, 2105-2113.

Montcouquiol, M., Sans, N., Huss, D., Kach, J., Dickman, J. D., Forge, A., Rachel, R. A., Copeland, N. G., Jenkins, N. A., Bogani, D. et al. (2006). Asymmetric localization of Vangl2 and Fz3 indicate novel mechanisms for planar cell polarity in mammals. *J. Neurosci.* **26**, 5265-5275.

Murdoch, J. N., Doudney, K., Paternotte, C., Copp, A. J. and Stanier, P. (2001). Severe neural tube defects in the loop-tail mouse result from mutation of Lpp1, a novel gene involved in floor plate specification. *Hum. Mol. Genet.* **10**, 2593-2601.

Park, M. and Moon, R. T. (2002). The planar cell-polarity gene stbm regulates cell behaviour and cell fate in vertebrate embryos. *Nat. Cell Biol.* **4**, 20-25.

Park, T. J., Haigo, S. L. and Wallingford, J. B. (2006). Ciliogenesis defects in embryos lacking inturned or fuzzy function are associated with failure of planar cell polarity and Hedgehog signaling. *Nat. Genet.* **38**, 303-311.

Petersen, C. P. and Reddien, P. W. (2009). Wnt signaling and the polarity of the primary body axis. *Cell* **139**, 1056-1068.

Philipp, I., Aufschnaiter, R., Özbek, S., Pontasch, S., Jenewein, M., Watanabe, H., Rentzsch, F., Holstein, T. W. and Hobmayer, B. (2009). Wnt/beta-catenin and noncanonical Wnt signaling interact in tissue evagination in the simple eumetazoan Hydra. *Proc. Natl. Acad. Sci. USA* **106**, 4290-4295.

Qian, D., Jones, C., Rzadzinska, A., Mark, S., Zhang, X., Steel, K. P., Dai, X. and Chen, P. (2007). Wnt5a functions in planar cell polarity regulation in mice. *Dev. Biol.* **306**, 121-133.

Roszko, I., Sawada, A. and Solnica-Krezel, L. (2009). Regulation of convergence and extension movements during vertebrate gastrulation by the Wnt/PCP pathway. *Semin. Cell Dev. Biol.* **20**, 986-997.

Seifert, J. R. K. and Mlodzik, M. (2007). Frizzled/PCP signalling: a conserved mechanism regulating cell polarity and directed motility. *Nat. Rev. Genet.* **8**, 126-138.

Simons, M. and Mlodzik, M. (2008). Planar cell polarity signaling: from fly development to human disease. *Annu. Rev. Genet.* **42**, 517-540.

Tsuji, T., Ohta, Y., Kanno, Y., Hirose, K., Ohashi, K. and Mizuno, K. (2010). Involvement of p114-RhoGEF and Lfc in Wnt-3a- and dishevelled-induced RhoA activation and neurite retraction in N1E-115 mouse neuroblastoma cells. *Mol. Biol. Cell* **21**, 3590-3600.

Vladar, E. K., Antic, D. and Axelrod, J. D. (2009). Planar cell polarity signaling: the developing cell's compass. *Cold Spring Harb. Perspect. Biol.* **1**, a002964.

Wallingford, J. B. (2010). Planar cell polarity signaling, cilia and polarized ciliary beating. *Curr. Opin. Cell Biol.* **22**, 597-604.

Wallingford, J. B. and Mitchell, B. (2011). Strange as it may seem: the many links between Wnt signaling, planar cell polarity, and cilia. *Genes Dev.* **25**, 201-213.

Wang, Y. and Nathans, J. (2007). Tissue/planar cell polarity in vertebrates: new insights and new questions. *Development* **134**, 647-658.

Wang, Y., Guo, N. and Nathans, J. (2006). The role of Frizzled3 and Frizzled6 in neural tube closure and in the planar polarity of inner-ear sensory hair cells. *J. Neurosci.* **26**, 2147-2156.

Wikramanayake, A. H., Hong, M., Lee, P. N., Pang, K., Byrum, C. A., Bince, J. M., Xu, R. and Martindale, M. Q. (2003). An ancient role for nuclear beta-catenin in the evolution of axial polarity and germ layer segregation. *Nature* **426**, 446-450.

Yin, C., Kiskowski, M., Pouille, P. A., Farge, E. and Solnica-Krezel, L. (2008). Cooperation of polarized cell intercalations drives convergence and extension of presomitic mesoderm during zebrafish gastrulation. *J. Cell Biol.* **180**, 221-232.

Zallen, J. A. (2007). Planar polarity and tissue morphogenesis. *Cell* **129**, 1051-1063.